Aptamer Antagonists of Myelin Promote Axon Growth

Presented by: Yuxuan Wang

In partial fulfillment of the requirements for graduation with the
Dean's Scholars Honor's Degree in Biochemistry

_____ _____

Dr. Andrew D. Ellington — Date
Supervising Professor

_____ _____

Dr. John F. Stanton — Date
Honor's Advisor in Biochemistry

TABLE OF CONTENTS

ABSTRACT

Myelin of the adult central nervous system (CNS) is one of the major sources of inhibition to axon regeneration following injury. The three known myelin-derived inhibitors (Nogo, MAG, and OMgp) bind with high affinity to the Nogo-66 receptor (NgR) on axons to limit neurite outgrowth. Here, we show that RNA aptamers can be generated that bind to NgR, compete with these inhibitors for binding to NgR, and promote axon elongation of neurons *in vitro* in the presence of these inhibitors. Aptamers have key advantages over protein antagonists, such as low cost and ease of production, high specificity and affinity for a wide range of targets, and simplicity with which they can be chemically modified to increase stability *in vivo*. The ability of aptamers to stimulate neurite elongation opens the possibility of reversing the inhibitory influence of CNS myelin via nucleic acid ligands.

INTRODUCTION

Patients with spinal cord injury suffer from permanent functional deficits and paralysis due to the limited capacity of axons to regenerate. Unlike their counterparts in the peripheral nervous system (PNS), damaged axons in the central nervous system (CNS) do not regenerate spontaneously because of an inhibitory environment. Studies have shown that CNS myelin is a major source of inhibition to axon regeneration (Fournier et al., 2001; Domeniconi et al., 2002; K. C. Wang et al., 2002). Trauma to the CNS can result in major disruptions in white matter tracts, including breakdown of myelin sheaths. Products of this myelin breakdown come in contact with the surfaces of severed axons and inhibit regeneration. The three known major myelin-derived inhibitors are Nogo-A, myelin-associated glycoprotein (MAG), and

oligodendrocyte myelin glycoprotein (OMgp). All three bind with high affinity to the Nogo-66 receptor (NgR) on axonal surfaces (Fournier et al., 2001; Domeniconi et al., 2002; K. C. Wang et al., 2002). Enzymatic cleavage of NgR confirms this effect, in that it increases axon regeneration (Fournier et al., 2001). Because NgR is a GPI-linked receptor and lacks an intracellular signaling domain, it relies on the transmembrane co-receptor, p75, to transduce the inhibitory signal. The final step in the signaling pathway is the activation of RhoA, a small GTPase that regulates actin polymerization and inhibits axonal elongation in its active form. Nogo-A, MAG, and OMgp activate RhoA through the NgR/p75 receptor complex, and this NgR/p75-complex/RhoA pathway is postulated to be responsible for the inhibitory signals that prevent axon regeneration (Yamashita and Tohyama, 2003).

Recent pharmacological methods to overcome CNS myelin inhibition involved the use of an anti-Nogo antibody (Schnell and Schwab, 1990; Bregman et al., 1995), RhoA inhibitors (Dergham et al., 2002; Fournier et al., 2003), a NgR antagonist peptide (GrandPre et al., 2002), and soluble NgR (Li et al., 2004).

There are potential problems with these inhibitors as therapeutic agents. For example, the direct blockade of RhoA with an inhibitor may disrupt other, crucial Rho-related cellular activities. In contrast, the anti-Nogo antibodies are only specific for Nogo and do not disrupt MAG or OMgp action. Because of this, it may be useful to identify high affinity inhibitors that more generally interact with the surface of NgR.

Aptamers are single-stranded oligonucleotides that fold into unique three-dimensional structures, allowing them to bind to protein targets with high affinity and specificity. They are considered as an alternative to therapeutic antibodies by offering the same advantages of antibodies but can be chemically synthesized in a cell-free system. Furthermore, aptamers have

a number of advantages over peptide and protein antagonists, including their relatively low cost of production, ease of GMP manufacture, and the simplicity with which they can be modified for signaling, immobilization, and stability (Jayasena, 1999; Rimmele, 2003; Nimjee et al., 2005; Lee et al., 2006). Clinical studies have shown that aptamers have no or low immunogenicity, and are generally non-toxic (Eyetech Study Group, 2002; Eyetech Study Group, 2003), which is a great advantage in comparison to antibodies given the length of treatment period required for spinal cord injuries. For example, Macugen, a pegylated 2-fluoro pyrimidine RNA aptamer and a potent inhibitor of the angiogenic regulatory protein, VEGF(165) (Cunningham et al., 2005; Ng and Adamis, 2005; Siddqui and Keating, 2005), was approved by the FDA for treatment of neovascular age-related macular degeneration in 2004.

Here, we selected RNA aptamers that bind to NgR with high specificity and affinity. Most importantly, these aptamers were shown to compete with Nogo, MAG, and OMgp for binding to NgR. Neurite outgrowth assays demonstrated that these aptamers can reverse the effect of these inhibitors *in vitro.*

RESULTS AND DISCUSSION

Selection of Anti-NgR aptamers

A RNA pool containing 50 randomized positions (R50) flanked by two constant, primer-binding regions was used as a starting point for selection. The protein target was a fusion of the extracellular domain of NgR and the constant region of IgG. In each round of selection, RNA-binding species were separated from weak or non-binding species by passing the protein:nucleic acid complexes through a modified nitrocellulose filter. Captured species were amplified via reverse transcription and PCR. Negative selections were carried out to remove sequences that bound species (the filter, IgG, and BSA) other than the target. Iterative rounds of selection and

amplification were performed until the target-binding sequences dominated the selected population.

Binding progressively increased and saturated at round 10. The selected population showed good specificity for NgR (36% RNA binding at 1 μM protein concentration), with little binding to BSA, IgG, or the filter (<1% RNA binding at 1 μM protein concentrations). The population was cloned and sequenced, and a best-binding, dominant sequence (Clone 6) was identified. To further improve affinity, additional variants were selected from a partially randomized pool based on Clone 6 that contained 70% wild-type and 30% non-wild type nucleotides. This level of mutagenesis should allow the accumulation of not only additional functional residues, but also changes in or additions to base-paired structures. In addition, a new selection was carried out with a slightly longer pool (N62) in order to identify aptamers that might cover larger swaths of the NgR surface and thereby prevent binding of multiple inhibitors. At the conclusion of both selections, 58 clones were sequenced: 29 from the Clone 6 doped re-selection, and 29 from the N62 selection. As expected, the best ligands for NgR were present multiple times in the selected populations (**Table S1**). However, no strong consensus sequences or motifs emerged from either selection. The diversity of aptamer sequences could mean that the selected aptamers interact in several different ways with NgR, a result that is consistent with the fact that very different myelin-derived inhibitors all bind to NgR.

The best aptamers were selected after a competition assay that identified binders with the highest affinity for relatively non-overlapping sites (**Figure S1**). The fact that the aptamers seemed to bind to non-overlapping sites on NgR is consistent with the selection of multiple, different sequences from both the original and doped sequence selections. The selected aptamers bound NgR with K_d values from 21 to 61 nM (**Table 1; Figure S2**). In comparison,

anti-Nogo antibodies bind to Nogo with K_d values of 8 μM and 1μM, for the wild-type and engineered II.1.8 mutant, respectively (Fiedler et al., 2002); while the NgR antagonist peptide NEP 1-40 shows half-maximum inhibition at 50nM (GrandPre et al., 2002).

Aptamers generally block inhibitor binding to NgR

The predicted protein structure of NgR includes a signal sequence, eight central leucine-rich repeats (LRRs) flanked by a cysteine-rich C-terminal subdomian (LRRCT) and a smaller leucine-rich N-terminal subdomain (LRRNT) (Fournier et al., 2001; Barton, et al; 2003). Studies suggest that all three inhibitors (MAG, Nogo, and OMgp) bind overlapping sites in the LRR repeat domains (Domeniconi et al., 2002; Wang et al., 2002). For example, NEP1-40 peptide can significantly, but only partially block myelin inhibition (GrandPre et al., 2002). This is because the peptide antagonist only blocks Nogo-66 mediated activity but not that of MAG (Fournier et al., 2002; Liu et al., 2002).

To determine whether or not the aptamers could more generally interfere with inhibitor binding than did other reagents, we assayed five of the best binding sequences in competition with Nogo, MAG, and OMgp. Remarkably, aptamers blocked more than one inhibitor simultaneously, and a modest diminution of aptamer binding (3-10 fold) was only seen at the highest total inhibitor concentration (3200nM) (**Figure 1**). As might be expected, there was a direct correlation between the affinity of the aptamers for NgR and the ability of the aptamers to compete with inhibitors for binding. The sequences with the lowest binding constants, Clone 40 and Clone 83, also showed the lowest decrease in binding in the presence of the inhibitors.

Aptamers localize to NgR-expressing neuronal and non-neuronal cell surfaces

Microscopy confirmed the binding of fluorescently-labeled aptamers to dissociated dorsal root ganglia (DRG), which have previously been shown to express NgR on their surfaces (Ahmed et al., 2006). After staining with a neuron-specific anti-beta III tubulin antibody, we found NgR expression in non-neuronal cell types in addition to DRG neurons (data not shown). To determine the nature of these non-neuronal, NgR-expressing cells, we stained the culture with an anti-S100 antibody, which identifies Schwann cells. The co-localization of the anti-NgR aptamers with the anti-S100 antibody suggested that NgR is expressed on Schwann cells. This discovery was further confirmed with an anti-NgR antibody, which again bound both neurons and Schwann cells (**Figure 2**). There was little to no binding to a cell line (A431) that lacked NgR, although the 431 cells were readily stained with a positive control, an anti-EGFR aptamer (**Figure S3**).

The localization of anti-NgR aptamers and antibody to Schwann cell surface led us to speculate the role of NgR on these cells. Schwann cells form the basis for nerve regeneration and repair in the PNS. Upon losing contact with axons such as following injury, mature Schwann cells undergo developmental regression and proliferation to provide an environment inductive to axonal re-growth (Fawcett and Keynes; 1990). However, Schwann cells were previously reported to express neither Nogo nor its receptor via *in situ* hybridization (Josephson, et al., 2002). The difference between previous and our own findings might the age-dependent expression of NgR in Schwann cells. The rat pups used in our experiments were newborns; whereas the mice pups used in the previous study were postnatal day 7. NgR expression might be downregulated as the animals reach adulthood, as previously observed in the spinal cord for humans and mice (Josephsen, et al., 2002).

Studies have shown that the lack of regeneration in the CNS is due to a hostile environment. For example, injured CNS axons can extend over long distances in the presence of a peripheral nerve graft (David and Aguayo, 1981). Given that PNS is significantly more permissive for growth relative to the CNS and that Schwann cells have a role in inducing axonal re-growth in the PNS, it is possible that these surface receptors act as competitive binders for myelin-derived inhibitors that might otherwise come in contact with growing axons. Indeed, given the larger number of Schwann cells it is possible that they act as a 'buffer' for the varying amounts of myelin-derived inhibitors that may be released. It is also interesting that these supporting cells express both NgR and myelin-proteins, such as MAG, but not Nogo and OMgp (Owens et al., 1990). This suggests an interesting scenario in which early Schwann cells can express both inhibitors of neurite growth and proteins that will bind the inhibitors, allowing the concentrations of these inhibitors to be very finely tuned in order to fine-tune neurite outgrowth over time.

Disinhibition of neurite outgrowth

To the extent that aptamers can compete with the inhibitors Nogo, MAG, and OMgp for binding to NgR, they were likely to show one of two biological effects: potentiation of neurite outgrowth (due to inhibition of the inhibitors) or inhibition of neurite outgrowth (due to mimicking of the inhibitors). To choose between these hypotheses, dorsal root ganglia (DRG) were isolated from P1-P3 rats and dissociated into single cells. The primary cultures included neurons and non-neuronal cells, such as Schwann cells. Throughout the study, the mitotic inhibitor 5-fluoro-2'-deoxyuridine (5-FDU) was added to arrest proliferation of non-neuronal cells.

In accordance with previous studies (Chen et al., 2000; Grandpre et al., 2000; Mukhopadhyay et al., 1994; McKerracher et al., 1994; Wang et al., 2002), the three myelin-derived inhibitors reduced axon elongation, as measured by the length of neurites formed in culture ($p<0.0001$). Approximately 200-500 cells were measured for each condition in triplicate (**Figure 3**). In contrast, the addition of aptamers increased growth significantly relative to the inhibitors-only control ($p<0.001$). Recovery of growth ranged 80-91% relative to the no-inhibitor control, almost a two-fold increase from full inhibition. Clone 83, the aptamer with the lowest binding constant, resulted in the highest reversal of inhibition among the aptamers, although at the concentrations assayed all of the aptamers showed similar effects on neurite outgrowth. In contrast, the negative control, random RNA sequences at the same concentration, did not affect axon elongation. Because all RNA samples were prepared at the same time using the same reagents and methods, this shows that the aptamers promoted neurite outgrowth based on their particular sequences alone.

Soluble NgR was used as a positive control and could also compete with inhibitors and increase neurite outgrowth (Li et al., 2004). The soluble receptor at 1μM, a concentration more than 3-fold that of the inhibitors, was not as effective as the aptamers in reversing the inhibition. A further disadvantage of the soluble NgR(310)ecto is that it only sequesters inhibitors in a one-to-one ratio whereas one aptamer could compete with the binding of multiple inhibitors (**Figure S4**).

ACKNOWLEDGEMENT

I especially owe my thanks to my advisor, Dr. Andrew Ellington, main collaborator, Dr. Zin Khaing, and her advisor, Dr. Christine Schmidt. I also thank my mentors, past and present, Drs. Na Li and Brad Hall. I am also thankful for the Freshman Research Initiative in the College of Natural Sciences, where my research first started.

This work was funded in part by the National Science Foundation and the Howard Hughes Medical Institute through the Freshman Research Initiative, and by the Gillson Longenbaugh Foundation. A portion of the images were colleced at the Microscopy and Imaging Facility of the Institute for Cellular and Molecular Biology at The University of Texas at Austin. We thank Dr. Wes Thompson and Dr. Raymond Grill for critical comments on the manuscript.

MATERIAL AND METHODS

In Vitro Selection

Aptamers against NgR were generated by *in vitro* selection, starting from synthetic DNA libraries. For the R50 pool, an oligonucleotide containing a 50-nucleotide random region (N50) flanked by constant regions was synthesized: 5'- GATAATACGACTCACTATAGGGTTTACCTAGGTGTAGATGCT-N50-AAGTGACGTCTGAACTGCTTCGAA-3'. The underlined portion is the T7 RNA polymerase promoter region. Similarly, the N62 pool consisted of a 62-nucleotide (N62) region flanked by a different pair of primers: 5' - GATAATACGACTCACTATAGGCGCTCCGACCTTAGTCTCTG-N62-GAACCGTGTAGCACAGCAGA - 3.' Following *in vitro* transcription by T7 RNA polymerase (Epicenter Technologies, Madison, WI), the derived RNA library was purified on an 8% denaturing polyacrylamide gel, then eluted and precipitated. In order to eliminate sequences from the population that bound to either the filter or the Fc region, an initial negative selection was carried out. The RNA population (~200 pmol, 10^{14} sequences) was incubated with 200 pmol of recombinant human IgG Fc (R&D Systems, Minneapolis, MN) and 0.01% BSA for 30 mins at 37^{o}C. Bound species were separated from unbound on a modified cellulose filter (Millipore, Bedford, MA). The sequences that passed through the filter were collected and then incubated with recombinant mouse Nogo receptor/Fc chimera (R&D Systems, Minneapolis, MN) in selection buffer (PBS, pH 7.4, 3mM $MgCl_2$) for 30 mins. Separation through a modified cellulose filter again trapped proteins and bound RNAs. After washing with 600µL Selection Buffer, RNA molecules were eluted from the filter in 200 nM NaCl, 50 mM Tris-

HCl, pH 7.4, 10 mM DTT, and 6 mM $MgCl_2$, and amplified by reverse transcription and the polymerase chain reaction (Invitrogen, Carlsbad, CA). An aliquot of the amplified DNA template (~1µg or 20 pmol, roughly one-sixth of total amount of amplicon produced) was used in a transcription reaction to generate an RNA pool for the subsequent round of selection. Iterative rounds of selection and amplification were performed until the target-binding sequences dominated the library population. In later rounds, the protein: RNA ratio, the $MgCl_2$ concentration, and the incubation time during the binding reaction were altered to increase stringency. The protein:RNA ration was 1:1 for the first two rounds, and 1:2 for subsequent rounds (protein was kept constant at 200 pmol, and RNA was varied from 200 to 400 pmol). The $MgCl_2$ concentration was 5mM for the first three rounds and 3mM for the subsequent rounds. The incubation time was 30 mins for the first three rounds and 20 mins for later rounds. Following sequencing, the MEME server [http://meme.sdsc.edu] was used to find potential sequence motifs.

Selections to optimize Clone 6, the dominant sequence from the initial selection (**Table S1**), were performed in a similar manner. The sequence for the partially randomized pool based on Clone 6 was 5'GGGTTTACCTAGGTGTAGATGCT*CTCTCTATTTCATTCGTAGGCTATTGGTGCCGCA AATACTAGCTTTACGA*AAGTGACGTCTGAACTGCTTCGAAAA - 3', where the italicized residues indicate positions that were synthesized at 70% wild-type and 30% non-wild-type nucleotides.

Binding Assays

The selected population was characterized for binding to NgR using a filter-binding assay similar to that used for the selection. The sequences were radioactively labeled in a transcription reaction using [α-^{32}P]ATP (3000ci/mmol, 10mCi/ml, Perkin Elmer, Waltham, MA). The labeled RNA was then incubated with 12.5, 18.75, 25, 37.5, 50, 75, 150, 300, and 500nM of the target protein (NgR/FC chimera). To separate the RNA bound to protein from free RNA, the reaction was passed through a nitrocellulose (top) then a nylon (bottom) filter (Schleicher & Schuell, Keene, NH) on a vacuum manifold. The nitrocellulose captured the RNA:protein complexes, while the nylon captured free RNA. After washing with Selection Buffer (600 µL), the filters were dried and exposed to a PhosphorImager plate (GE Healthcare, Piscataway, NJ) to quantitiate the amount of retained radioactivity. The fraction of a given RNA (population or aptamer) that bound the target proteins was calculated by comparing the counts retained on the filter with the total number of counts in the original RNA. Binding to IgG and BSA were assayed similarly. The maximum binding (B_{max}) and dissociation constants (K_d) were fit using the program SigmaPlot (Chicago, IL). The K_d curves were plotted in Sigma plot according to the following equation:

$$\text{RNA Bound} = \frac{B_{max}[\text{Protein}]}{K_d + [\text{Protein}]}.$$

Competition Binding Assays

Competition between aptamers and myelin-derived inhibitors was assayed by measuring the reduction in aptamer binding in the presence of the inhibitors. The aptamers were again radioactively labeled during transcription as described above. The NgR/Fc chimera (50 nM) was incubated with Nogo, MAG, and OMgp (R&D Systems, Minneapolis, MN, each at 200 nM or 800 nM) for 5 mins. Aptamers were then introduced and incubated with the mixture for 20 mins at 37^{o}C. The binding reaction was passed through filters on a vacuum manifold, and the filters were washed and quantified as described in the binding assays above. The fraction of RNA

bound was measured. Decreases in aptamer binding due the formation of inhibitor-NgR complexes were determined in comparison with an aptamer alone control.

Neurite Outgrowth Assays

Dorsal root ganglia (DRG) were removed from P1-P3 rats and trimmed to remove axons for accurate measurements of re-growth in RPMI (Sigma-Aldrich, St. Louis, MO). DRGs were dissociated into single cells by incubation with 0.25% collagenase type I (Sigma-Aldrich) at 37^{o}C for 30 mins and 0.025% trypsin (Sigma-Aldrich, St. Louis, MO) for 37 ^{o}C for 10 mins. Dulbecco's Modified Eagle's Medium (Sigma-Aldrich) with 10% fetal bovine serum (Hyclone, Logan, UT) and 1% penicillin-streptomycin (Sigma-Aldrich) was added to dissociated cells, and the cells were plated in 24-well plates coated with 50 µg/ml poly-L-lysine (Sigma-Aldrich, St. Louis, MO) and 10 µg/ml laminin (Trevigen, Gaithersburg, MD) at a density of 50,000 cells/well. At the time of plating, 30 nM of 5-fluoro-2'-deoxyuridine (Sigma-Aldrich) was added to arrest proliferation of non-neuronal cell types. The three myelin-derived inhibitors (each at a final concentration 100 nM), RNAse inhibitors at 1.6 Units/µl (Ambion, Austin, TX), and a given RNA (final concentration 10 µM) were added an hour after plating (to minimize interference with cell adherence). After 24 hours of incubation, the cells were fixed in 4% paraformaldehyde, immunostained with a neuron-specific anti-β-tubulin III antibody (Abcam, Cambridge, MA) and an Alexa Fluor 488-labeled goat anti-rabbit IgG (Invitrogen, Carlsbad, CA) as the secondary antibody. To assay the impact of compounds on neurite outgrowth the lengths of individual immunostained neurites were measured. The cell density and growth time were optimized to ensure that neurons grew in relative isolation from each other and that neurites from nearby cells did not fasciculate. An inverted fluorescence microscope (IX-70, Olympus) was used to visualize the cells, and images from the microscope were acquired using a color CCD video camera (Optronics Magna-Fire, model S60800). Quantification of neurite outgrowth was performed over a sample of 200-500 neurons per condition using Leica QWIN Image Analysis software (Leica Microsystems, Bannockburn, IL). Gray image processing was first used to identify all anti-β-tubulin III-stained neurons. Cell bodies were subsequently removed using BINARY EDIT functions. The curve lengths (defined as the length of the longest side of a rectangle having the same area and perimeter as the measured feature) of the remaining neurites on 200-500 neurons were measured and averaged. The significance of the collected data was assessed using a pairwise t-test with Bonferroni correction (**Table S2**).

Aptamer Localization

In order to better label the aptamers, a 3' extension was added by PCR. The extensions were 5' *CTGGTCATGGCGGGCATTTAATTC*TTCGAAGCAGTTCAGACGTCACTT 3' for the R50 pool; and 5' *CTGGTCATGGCGGGCATTTAATTC*TCTGCTGTGCTACACGGTTC 3' for the N62 pool. The italicized portions indicate regions of complementarity to a biotinylated oligonucleotide. RNAs (1 µM) transcribed from the extended templates were purified and hybridized to the biotinylated oligonucleotide (5' GAATTAAATGCCCGCCATGACCAG *3'*) (1 µM) by heating to 70^{o}C for 3 mins and cooling to 25^{o}C. The RNA:DNA hybrid was further incubated with streptavidin:phycoerythrin (PE) (1uM) to generate fluorescent complexes. Dissociated DRGs were prepared as described above. The entire aptamer:biotinylated oligonucleotide:streptavidin:PE complex was incubated with the dissociated DRG culture for 30 mins in the presence of RNAse inhibitors at 1.6 units/µl (Ambion, Austin, TX). The DRGs were then washed 3 times with selection buffer (PBS + 3 mM $MgCl_2$), fixed in 4% paraformaldehyde,

and immunostained with a neuron-specific anti-β-tubulin III antibody (Abcam, Cambridge, MA) or an anti-S100 antibody (Abcam, Cambridge, MA) and an Alexa Fluor 488-labeled goat anti-rabbit IgG (Invitrogen, Carlsbad, CA) as the secondary antibody. Staining with a biotinylated anti-NgR antibody (R&D Systems, Minneapolis, MN) was performed similarly, except that the antibody was conjugated to streptavidin:PE. Fluorescence images were collected using a Leica SP2 AOBS confocal microscope. The brightness and contrast of images were enhanced in Adobe Photoshop (Adobe, San Jose, CA) to optimize visualization.

REFERENCES

Fournier AE, GrandPre T & Strittmatter SM (2001). Identification of a receptor mediating Nogo-66 inhibition of axonal regeneration. Nature 409:341–346.

Domeniconi M, Cao Z, Spencer T, Sivasankaran R, Wang K, Nikulina E, Kimura N, Cai H, Deng K, Gao Y, He Z, Fibin M (2002). Myelin-associated glycoprotein interacts with the Nogo-66 receptor to inhibit neurite outgrowth. Neuron 35:283–90.

Wang KC, Kim JA, Sivasankaran R, Segal R, He Z (2002). P75 interacts with the Nogo receptor as a co-receptor for Nogo, MAG, and OMgp. Nature 420:74–78.

Yamashita T, Tohyama M (2003). The p75 receptor acts as a displacement factor that releases Rho from Rho-GDI. Nature Neurosci. 6:461–467.

Schnell L, Schwab ME (1990). Axonal regeneration in the rat spinal cord produced by an antibody against myelin-associated neurite growth inhibitors. Nature 343:269–272.

Bregman BS, Kunkel-Bagden E, Schnell L, Dai HN, Gao D, Schwab ME (1995). Recovery from spional cord injury mediated by antibodies to neuurite growth inhibitors. Nature 378: 498-501.

Dergham P, Ellezam B, Essagian C, Avedissian H, Lubell WD, McKerracher L (2002). Rho signaling pathway targeted to promote spinal cord repair. J. Neurosci. 22:6570–6577.

Fournier AE, Takizawa BT, Strittmatter SM (2003). Rho kinase inhibition enhances axonal regeneration in the injured CNS. J Neurosci 23:1416-1423.

GrandPre T, Li S, Strittmatter SM (2002). Nogo-66 receptor antagonist peptide promotes axonal regeneration. Nature 417:547–551.

Li S, Liu BP, Budel S, Li M, Ji B, Walus L, Li W, Jirik A, Rabacchi S, Choi E, Worley D, Sah DWY, Pepinsky B, Lee D, Relton J, Strittmatter SM (2004). Blockade of Nogo-66, Myelin-associated glycoprotein, and oligodendrocyte myelin glycoprotein by soluble Nogo-66 receptor promotes axonal sprouting and recovery after spinal injury. J. Neurosci. 24 (46):10511-10521.

Jayasena SD (1999). Aptamers: an emerging class of molecules that rival antibodies in diagnostics. Clin Chem 45: 1628-1650.

Rimmele M (2003). Nucleic acid aptamers as toold and drugs: recent developments. Chembiochem 4: 963-971.

Nimjee SM, Rusconi CP, Sullenger BA (2005). Aptamers: an emerging class of therapeutics. Annu Rev Med 56: 555-583.

Lee J, Stovall G, Ellington A (2006). Aptamer therapeutics advance. Curr. Opin. Chem. Biol. 10:282–289.

Eyetech Study Group (2002). Preclinical and phase 1A clinical evaluation of an anti-VEGF pegylated aptamer (EYE001) for the treatment of exudative age relative macular degeneration. Retina 22:143-152.

Eyetech Study Group (2003). Antivascular endothelial growth factor therapy for subfoveal choroidal neovascularization secondary to age related macular degeneration: Phase II study results. Ophthalmology 110:979–986.

Cunningham ET Jr, Adamis AP, Altaweel M, Aiello LP, Bressler NM, D'Amico DJ, Goldbaum M, Guyer DR, Katz B, Patel M, Schwartz SD; Macugen Diabetic Retinopathy Study Group (2005). A phase II randomized double-masked trial of pegaptanib, an anti-vascular endothelial growth factor aptamer, for diabetic macular edema. Ophthalmology 112:1747-1757.

Ng EW, Adamis AP (2005). Targeting Angiogenesis, the underlying disorder in neovascular age-related macular degeneration. Can J Ophthalmol 40:352-358.

Siddqui MA, Keating GM (2005). Pegaptanib in exudative age-related macular degeneration. Drugs 65:1571–1577, discussion 1578–1579.

Barton WA, Liu BP, Tzvetkova D, Jeffrey PD, Fournier AE, Sah D, Cate R, Strittmatter SM, Nikolov DB (2003). Structure and axon outgrowth inhibitor binding of the Nogo-66 receptor and related proteins. EMBO J. 22:3291-302.

Wang KC, Koprivica V, Kim JA, Sivasankaran R, Guo Y, Neve RL, He Z (2002). Oligodendrocyte-myelin glycoprotein is a Nogo receptor ligand that inhibits neurite outgrowth. Nature 417, 941–944.

Fiedler M, Horn C, Bandtlow C, Schwab ME, Skerra A (2002). An engineered IN-1 F(ab) fragment with improved affinity for the Nogo-A axonal growth inhibitor permits immunochemical detection and shows enhanced neutralizing activity. Protein Eng 11:931-41.

Fournier AE, GrandPre T, Gould G, Wang X, Strittmatter SM (2002). Nogo and the Nogo-66 receptor. Prog Brain Res 137:361-369.

Liu BP, Fournier A, GrandPré T, Strittmatter SM (2002). Myelin-associated glycoprotein as a functional ligand for the Nogo-66 receptor. Science. 297:1190-3.

Ahmed Z, Mazibrada G, Seabright RJ, Dent RG, Berry M, Logan A (2006). TACE-induced cleavage of NgR and p75NTR in dorsal root ganglion cultures disinhibits outgrowth and promotes branching of neurites in the presence of inhibitory CNS myelin. FASEB J. 11,1939-41.

Fawcett JW, Keynes RJ (1990). Peripheral nerve regeneration. Annu Rev Neurosci 13:43-60.

Josephson A, Trifunovski A, Widmer HR, Widenfalk J, Olson L, Spenger C (2002). Nogo-receptor gene activity: cellular localization and developmental regulation of mRNA in mice and humans. J Comp Neurol.453:292-304.

David S, Aguayo, AJ (1981). Axonal elongation into peripheral nervous system 'bridges' after central nervous system injury in adult rats. Science 214, 931–933.

Owens GC, Boyd CJ, Bunge RP, Salzer JL (1990). Expression of recombinant myelin-associated glycoprotein in primary Schwann cells promotes the initial investment of axons by myelinating Schwann cells. J. Cell Biology 111:1171-1182.

Chen MS, Huber AB, van der Haar ME, Frank M, Schnell L, Spillmann AA, Christ F, Schwab ME (2000). Nogo-A is a myelin-associated neurite outgrowth inhibitor and an antigen for monoclonal antibody IN-1. Nature 403, 434–439.

GrandPre T, Nakamura F, Vartanian T, Strittmatter SM (2000). Identification of the Nogo inhibitor of axon regeneration as a Reticulon protein. Nature 403, 439–444.

Mukhopadhyay G, Doherty P, Walsh FS, Crocker PR. & Filbin MT (1994). A novel role for myelin-associated glycoprotein as an inhibitor of axonal regeneration. Neuron 13, 757–767.

McKerracher L, David S, Jackson DL, Kottis V, Dunn RJ, Braun PE (1994). Identification of myelin-associated glycoprotein as a major myelin-derived inhibitor of neurite growth. Neuron 13, 805–811.

FIGURES AND TABLES

Table 1

The sequences of the random regions of the aptamers tested in neurite outgrowth assays, maximum binding in our standard assay (B_{max}), and dissociation constants (K_d).

Clone	Sequence	B_{max}(%)	K_d(nM)
40	ATAACACGACATCCATATGTCAGTGGTCTGTGTACTTACACGGTATTCGA	81±7	25±8
79	ACTACACGAGGACCTACGACTACTACATTATGCCAACCGGTCTTGCTTCGACACAGATACCTC	85±8	60±16
83	TTGCACAAGATACGGCTACCTGTATGCGGCAATCGGCATTAAATCTATCTAAGCCAGCAGTAAC	65±3	21±4
110	ATAACACGACATCCATATGTCAGTGGTCTGTGTACGTACACGGTATTCGC	95±8	50±13
152	GGCGATAGTTTCTATAGCAAGGTACAGCATTCTCTCTCCCTATAGAACCAATCCAGTACTAGC	84±8	61±16

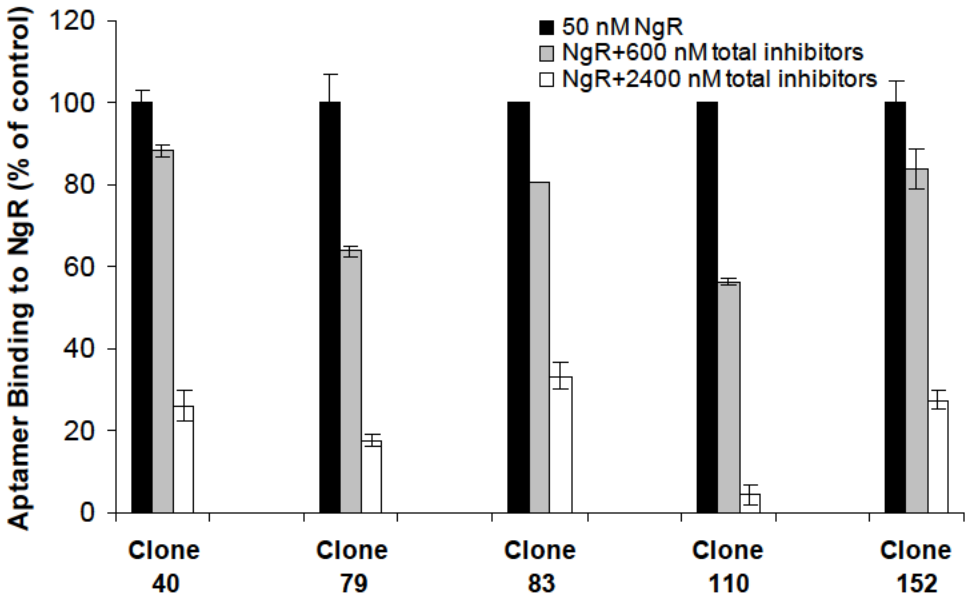

Figure 1. Competition assay between aptamers and myelin-derived inhibitors. The three myelin-derived inhibitors (Nogo, MAG, OMgp) at excess concentrations (200 or 800 nM for each of the three inhibitors, implying 600 and 2400 nM total inhibitor concentrations) reduced aptamer (5 nM) binding to NgR (50 nM) in a standard assay. Results were normalized to the aptamer alone controls. Binding data is the average of two determinations.

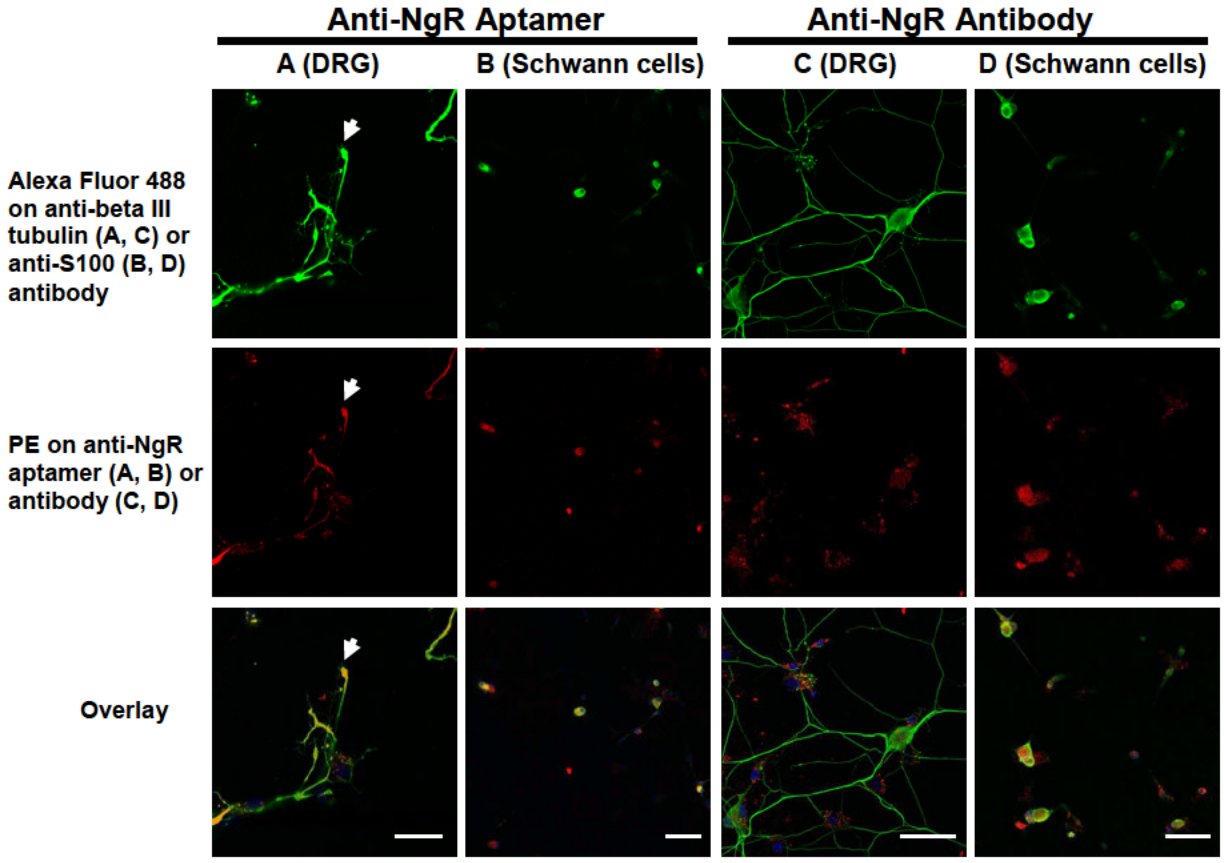

Figure 2. NgR expression in dorsal root ganglia and Schwann cells. DRG neurons in primary cultures were labeled using an anti-beta III tubulin antibody (green; columns A, C). Schwann cells were labeled using an anti-S100 antibody (green; columns B, D). Binding of a biotinylated anti-NgR aptamer (Clone 40) was detected with PE-labeled streptavidin (red; A, B). Binding of a biotinylated anti-NgR antibody was also detected with PE-labeled streptavidin (red; C, D). Yellow in the overlay indicates the overlap of green and red stains. Arrows in Column A indicate the position of a growth cone in a DRG neuron, and the overlay suggests localized expression of NgR. Scale bars: 25 µm (A); 50 µm (B-D).

A.

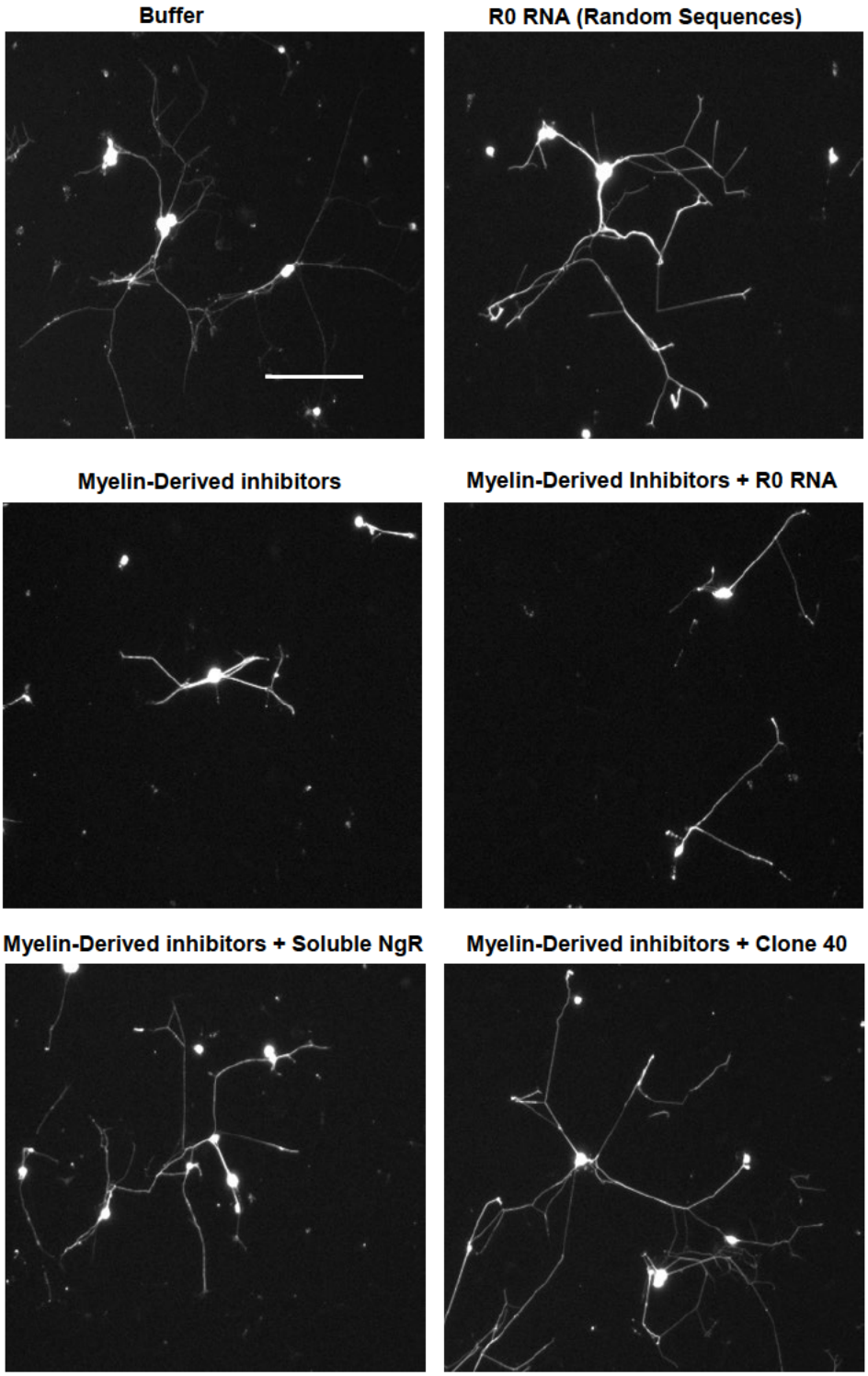
Buffer
R0 RNA (Random Sequences)
Myelin-Derived inhibitors
Myelin-Derived Inhibitors + R0 RNA
Myelin-Derived inhibitors + Soluble NgR
Myelin-Derived inhibitors + Clone 40

B.

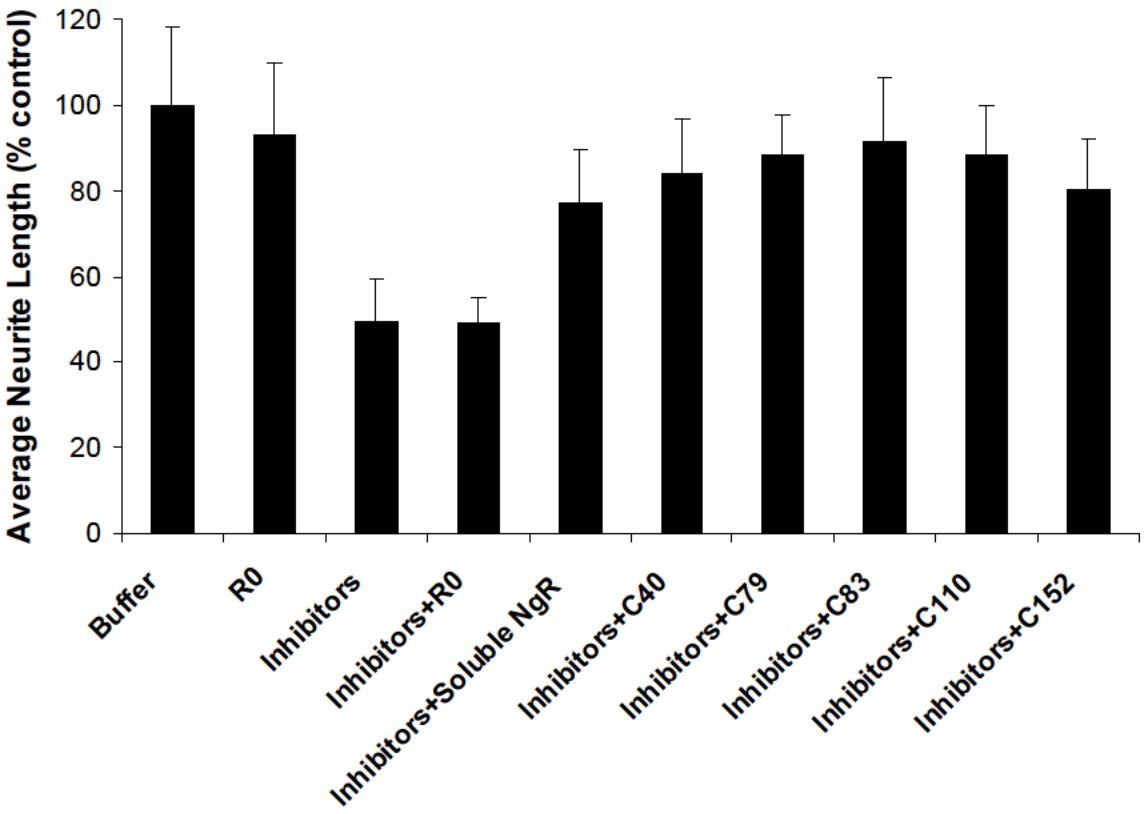

Figure 3. Neurite outgrowth assays with dorsal root ganglia. The myelin-derived inhibitors (Nogo, MAG, and OMgp) were added at 300 nM total (100 nM each). Aptamers (Clones 40, 79, 83, 110, and 152) were added at a concentration of 10 μM. (A) Visualization of neurite lengths. DRGs were stained with a neuron-specific anti-beta III tubulin antibody. The pictures shown are representative examples. Scale bar, 200 μm. (B) Average neurite lengths. Data was collected over 200-500 neurons per condition, and means + standard deviations are reported. Binding was normalized to a buffer alone control.

SUPPLEMENTARY TABLES AND FIGURES

Table S1. Aptamer sequences. The random regions of aptamers from the Clone 6 doped re-selection (A) and the N62 selection (B) are shown. Out of the 58 clones sequenced, there were 23 distinct sequences. Several 5-bp long motifs (colored) appeared in multiple aptamers. (*) indicates a high-affinity sequence, most of which appeared multiple times in the cloned population, and which were competed with one another to identify aptamers that bound to distinct regions on NgR (**Figure S1**). (**) indicates the highest affinity sequences that bound to relatively non-overlapping regions on NgR and that were further tested in neurite outgrowth assays (see also **Table 1**).

Clone	Sequence	Repeats
6(Initial Sequence)	CTCTCTATTTCATTCGTAGGCTATTGGTGCCGCAAATACTAGCTTTACGA	0
*27	CCTTATTCCCTAGTATACCAAGAGTGTTGTGTACTCCGCTTAGTATCCT	10
*45	GAATCCCGCTCTGTTTAATCCCGGCATCTCCAGGAATTATACCTACAAC	4
*39	TAAGCCCCAGTTTCATCGATAGTATTCGCATTGCGCTCAGCGAATGTA	4
108	TTGTCACTTTCGTCCCTAGGTTATTGTTGCCCCAAATAACTTCTTTTTA	2
105	CGCTGTTGTCCCTCCCTTGGAATCTACGGACAACCCACCCTACCTAGAGT	2
**40	ATAACACGACATCCATATGTCAGTGGTCTGTGTACTTACACGGTATTCGA	1
**110	ATAACACGACATCCATATGTCAGTGGTCTGTGTACGTACACGGTATTCGC	1
26	CTCGTGATTGTATTCGTAAGTCATTAGTTACGCAATTAATGATTTACAG	1
32	GATTTTATTTCAGTGTTAGGGTAGTCATTCCCTACATTCCACCTTTACTC	1
29	TAATCCCCAGTTTCATCGATAGTATTCGCATTGCGCTCAGCGAATGTA	1
30	TAACCCCCAGTTTCATCGATAGTATTCGCATTGCGCTCAGCGAATGTA	1
33	TTCTCACTTTCGTCCCTAGGTTATAGGTCCCACACATTCCCGCCCTACTA	1

A. R50 Doped Selection

Clone	Sequence	Repeats
**79	ACTACACGAGGACCTACGACTACTACATTATGCCAACCGGTCTTGCTTCGACACAGATACCTC	13
*81	ACAGCTAAACACATCTGTACGCGCGTTTACTAATACATGTTCTAAATAGACGTAGCGGTAAC	5
*82	TATTAATTCACTGTTTGCAGTTGCCTCCTGTTCGTTTACTCTTTACCCTTAAACGACAGCCT	2
**83	TTGCACAAGATACGGCTACCTGTATGCGGCAATCGGCATTAAATCTATCTAAGCCAGCAGTAAC	1
**152	GGCGATAGTTTCTATAGCAAGGTACAGCATTCTCTCTCCCTATAGAACCAATCCAGTACTAGC	1
78	ACTACGAGAGGACTTACGAATGAGACCATATGCCAACCGGTCTGGCTTCGACACAGATTCCTA	1
80	GGAAACCCTAAGATCTGAAATTAATCCTCCCAGTACTACTCAGAAAAAAAAACGCGACACAGCCC	1
85	CAGACGTAGCGAAAGAGGGCCTGGGTAGGTACTGACACGGGGATTCGCCTTACGTGGGACGT	1
88	AACACAGCTCCATGGACTTCTGAGTGGATGCGATCCATACTGGGATTAGCAGTGCCCTC	1
92	TCAATACACGCTGAAATAGCACTGATTAATCCCGCACCATGGGGCATGTGCGATGCCCCTGC	1
148	CCGAATGTCTTTGCTTCAACACTGTCAACTGTACGCGGCGTATATTCTACTCCAGCGGTAAC	1

B. N62 Selection

Table S2. P values obtained by pairwise t-test with Bonferroni correction. Aptamers significantly increased growth compared to the inhibitor-only control. Furthermore, the extent of outgrowth in aptamer-treated samples (Inh+C40, inh+C79, inh+C83, inh+C110) was statistically equivalent to that of the no-inhibitor control (Buffer).

	Buffer	**Inhibitors (Inh)**	**Inh+ sol NgR**	**Inh+C40**	**Inh+C79**	**Inh+C83**	**Inh+C110**
Inhibitors (Inh)	1.7e-15	--	--	--	--	--	--
Inh+ sol NgR	0.0036	6.4e-05	--	--	--	--	--
Inh+C40	0.1528	1.4e-08	1.0000	--	--	--	--
Inh+C79	1.0000	9.3e-11	1.0000	1.0000	--	--	--
Inh+C83	1.0000	1.8e-11	0.3207	1.0000	1.0000	--	--
Inh+C110	1.0000	1.4e-09	1.0000	1.0000	1.0000	1.0000	--
Inh+C152	0.0119	2.6e-07	1.0000	1.0000	1.0000	1.0000	1.0000

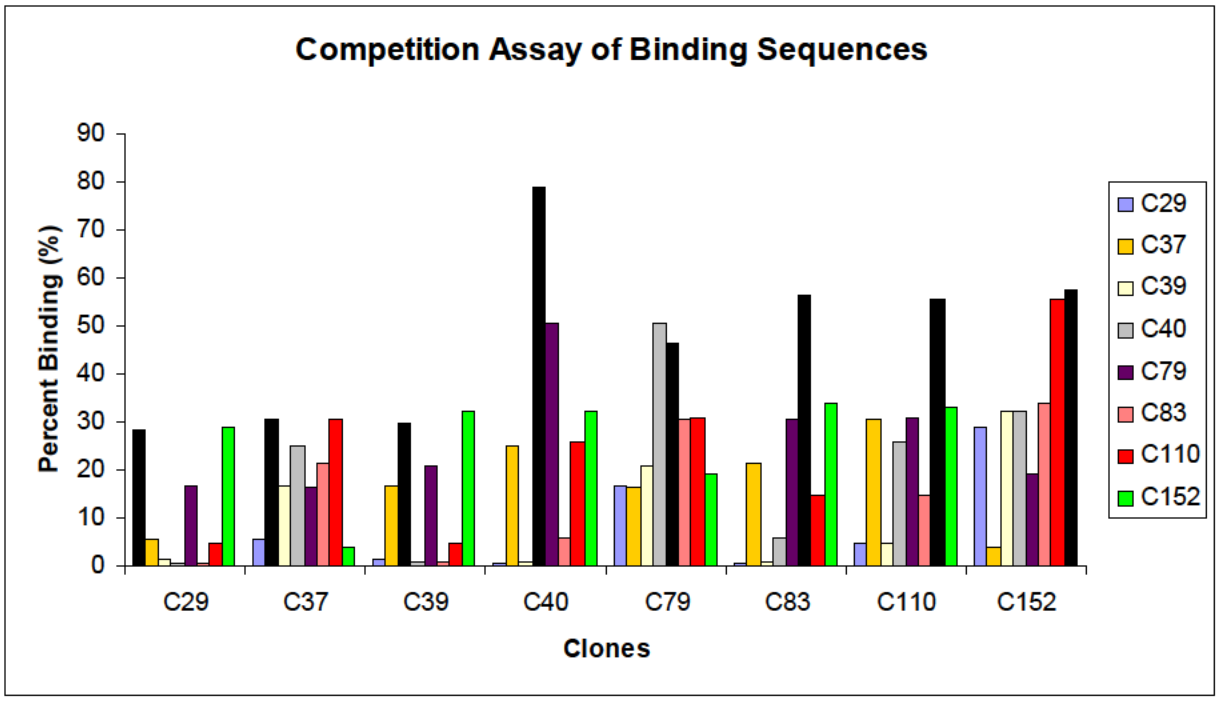

Figure S1. Competition between aptamers for binding to NgR. The highest affinity species from the original selections (**Table S1**) were chosen to compete with one another. Black denotes the binding of the radiolabeled aptamer (10nM) to NgR (100nM), without competition. Competition with against another aptamer (500nM; or 50:1 cold:radiolabeled aptamer) in our standard binding assay is shown with a different color. Based on these results, C29 and C39 were not further investigated, because they had similar specificity to but lower affinity than C40. Likewise, C37 bound similarly to C152.

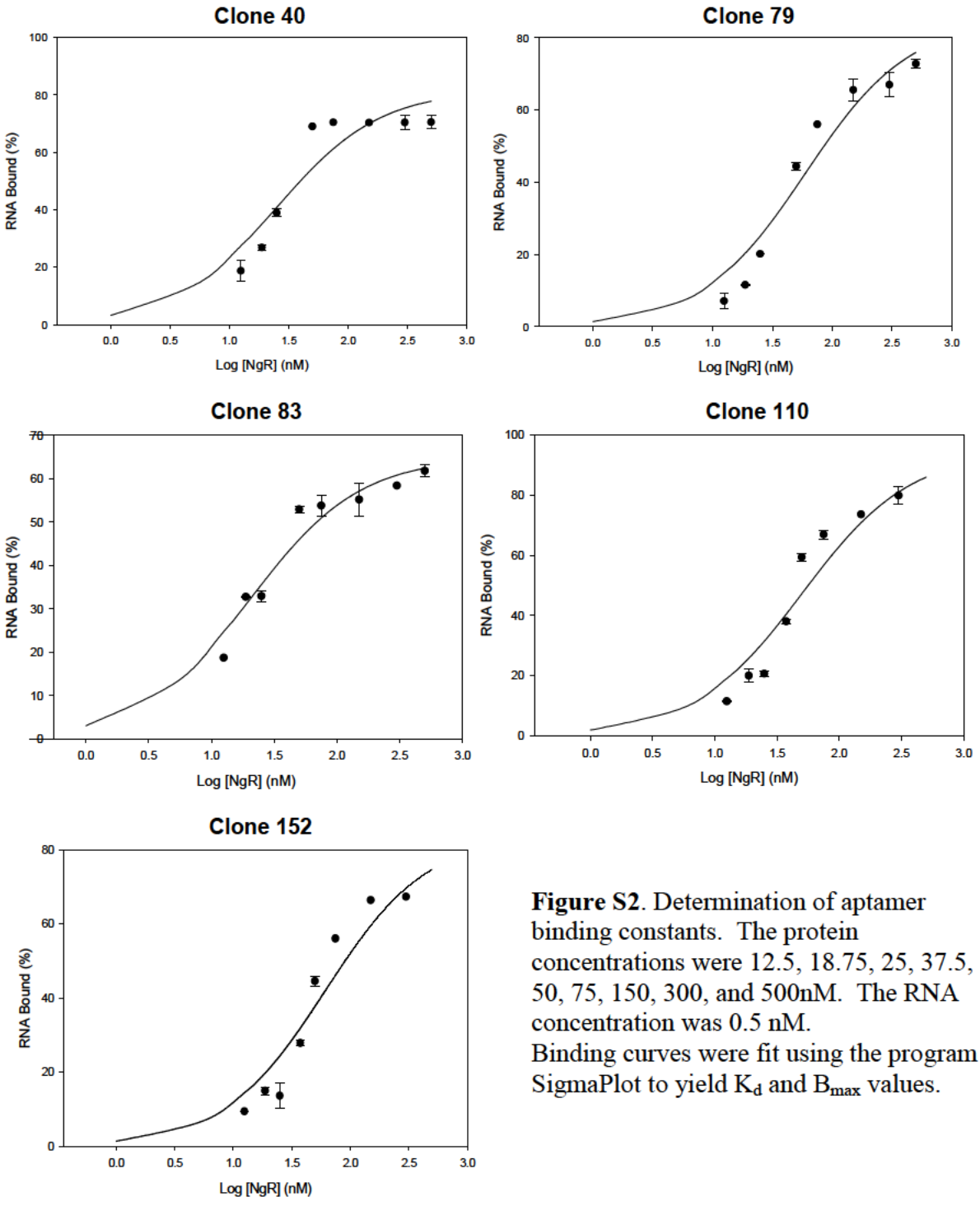

Figure S2. Determination of aptamer binding constants. The protein concentrations were 12.5, 18.75, 25, 37.5, 50, 75, 150, 300, and 500nM. The RNA concentration was 0.5 nM.
Binding curves were fit using the program SigmaPlot to yield K_d and B_{max} values.

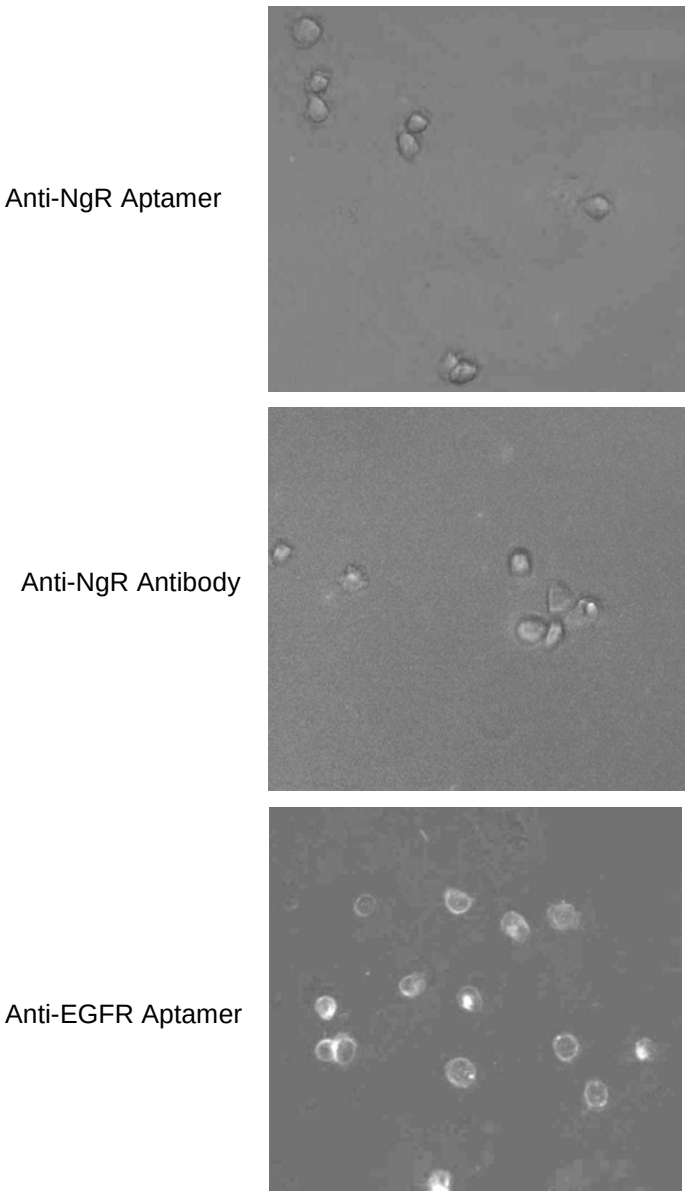

Figure S3. Anti-NgR aptamers are specific for neuronal cell lines. Biotinylated aptamers and antibodies were labeled using Alexa568 streptavidin. The human epithelial carcinoma tissue culture cell line A431 expresses EGFR (epidermal growth factor receptor) but not NgR. Thus an anti-NgR aptamer (Clone 40) and an anti-NgR antibody showed little binding to these cells (no bright spots, top two panels) relative to an anti-EGFR aptamer (bottom panel).

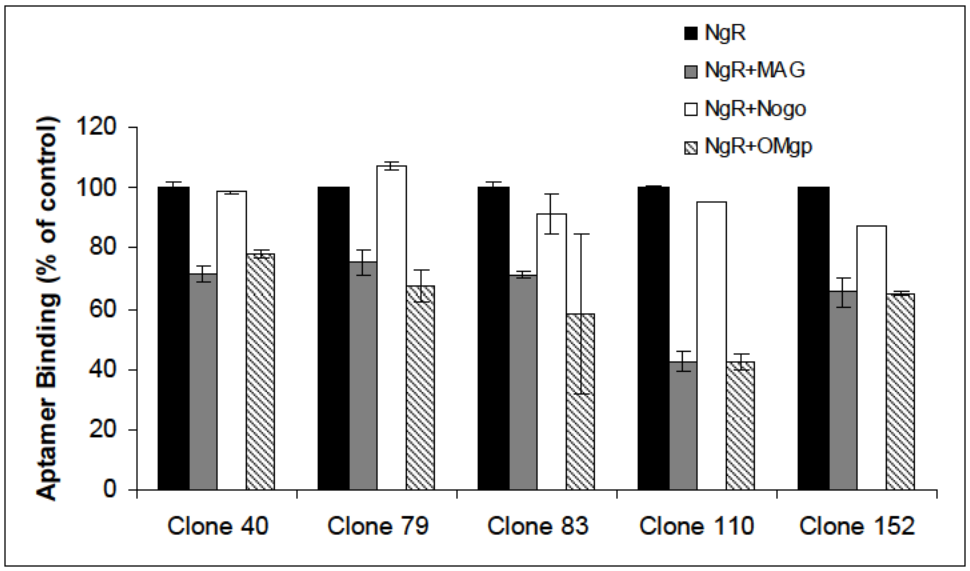

Figure S4. Competition between aptamers and individual myelin-derived inhibitors. The three myelin-derived inhibitors (Nogo, MAG, OMgp) at excess concentrations (800 nM each) were incubated with the aptamer (10 nM) and NgR (50 nM) in a standard binding assay. MAG and OMgp generally reduce aptamer binding. This suggests these inhibitors and aptamers bind to overlapping or identical sites on NgR. It should be noted that even though Nogo does not appear to compete with the aptamers, it also does not appear to be effective in reducing aptamer-stimulated neurite outgrowth (**Figure 3**), suggesting it may bind more weakly than aptamers to NgR.